Available online at www.sciencedirect.com

ScienceDirect

Procedia CIRP 94 (2020) 627–631

www.elsevier.com/locate/procedia

11th CIRP Conference on Photonic Technologies [LANE 2020] on September 7-10, 2020

Notch impact toughness of laser beam welded thick sheets of cryogenic nickel alloyed steel X8Ni9

S. Gook[a,*], S. Krieger[a], A. Gumenyuk[b], A. M. El-Batahgy[c], M. Rethmeier[a,b,d]

[a]*Fraunhofer Institute for Production Systems and Design Technology IPK, Pascalstraße 8-9, 10587, Berlin, Germany*

[b]*Federal Institute for Materials Research and Testing BAM, Unter den Eichen 87, 12205, Berlin, Germany*

[c]*Central Metallurgical R & D Institute CMRDI, P. O. Box: 87 Helwan, El-Tabbin, Cairo, Egypt*

[d]*Institut für Werkzeugmaschinen und Fabrikbetrieb IWF, Technische Universität Berlin, Straße des 17. Juni 135, 10623 Berlin, Germany*

* Corresponding author. Tel.: +49-30-39006-375 ; fax: +49-30-39110-37. *E-mail address:* sergej.gook@ipk.fraunhofer.de

Abstract

The paper deals with the investigations of the impact toughness of laser beam welded 14.5 mm thick sheets made of cryogenic steel X8Ni9 as a function of preheating. This 9% nickel alloyed steel is widely used in the liquefied natural gas (LNG) industry. An application of highly efficient welding processes such as high-power laser beam welding (LBW) in LNG sector requires an understanding of the interactions between the LBW process parameters and weld properties, in particular the impact toughness. The results show that the original fine-grained martensitic microstructure of the base metal (BM) is significantly changed by melting and crystallization during the LBW, what can lead to a decrease in the impact toughness of the weld metal (WM) below the required level. An optimal preheating temperature range leads to the favorable thermal welding cycle and is of remarkable importance for maintaining the notch impact toughness of laser beam welded joints of these thick steel sheets. A parameter window was identified in which V-notch impact toughness comparable to that of the BM at -196 °C was achieved.

*Keywords:*cryogenic steel, laser beam welding, preheating, welding thermal cycle, microstructure, hardness, V-notch impact toughness

1. Introduction

The cryogenic steel X8Ni9 is, according to A553 Type 1, a low-carbon nickel alloyed steel with a nominal nickel content of 9%. It is characterized by a high strength and excellent fracture toughness at low temperatures and is therefore used in particular for low-temperature applications in the LNG sector at operating temperatures of up to -196 °C [1, 2].

Generally, the sheets of X8Ni9 can be joined using arc-based welding procedures such as the shielded metal arc welding (SMAW), gas tungsten arc welding (GTAW), gas metal arc welding (GMAW) or submerged arc welding (SAW). These welding processes are robust, but the need to use relatively expensive austenitic Cr-Ni or Ni-based fillers has a significant negative economic impact on the construction costs of LNG facilities [3, 4]. This fact makes the introducing of highly efficient welding processes such as high power LBW for the LNG sector very important from an economic point of view in addition to productivity and quality.

The significance of this technological task for LNG has already been recognized and first investigations on the use of LBW and hybrid laser arc welding (HLAW) for joining of thick steel X8Ni9 have been initiated and carried out by various research groups [5-7]. It was shown in previous experiments that a V-notch impact toughness up to 1.0 J/mm^2 could be achieved for the LBW of 7.2 mm thick sheets X8Ni9 [8]. However, it was not readily possible to transfer results to a larger sheet thicknesses, particularly with regard to ensuring the required

10.1016/j.procir.2020.09.095

impact strength of the laser beam weld seam. A quite low V-notch toughness of 0.26 J/mm^2 has so far been achieved for the 14.5 mm thick sheets X8Ni9 [9].
The regulations of the International Classification Society Det Norske Veritas and Germanischer Lloyd (DNV GL) specify the required average energy of the Charpy V-notch impact test of 34 J (0.42 J/mm^2) for the welds on Ni-alloyed steels for LNG applications [10]. Some LNG project specifications often require a minimum impact toughness of 0.75 J/mm^2, which corresponds to the impact absorbed energy of 60 J at the test temperature of -196 °C [11].
The main difficulties with LBW of the X8Ni9 steel should be seen due to its complex phase and structure composition. This heat treated (quenched and tempered) steel has an increased nickel content and is therefore characterized by a fine-grained microstructure consisting of relatively soft nickel-martensite with a small amount of residual austenite. It is assumed that the reduction in toughness of the WM and HAZ of cryogenic nickel alloyed steels is caused mainly by coarse austenite grains which are formed during solidification of the weld pool, solidification segregation of nickel near the prior austenite grain boundaries and carbide particles, which are predominantly distributed along the grain boundaries, causing embrittlement [12-14]. It is therefore strongly recommended to control the heat input when welding the cryogenic X8Ni9 steel [11, 15].
The aim of the experiments presented in this paper is to clarify whether an adaptation of the welding thermal cycle has a positive effect on the impact toughness of the laser beam welded thick sheets made of heat treated cryogenic steel X8Ni9.

2. Experimental

2.1. Materials

The used BM is a commercial 9% nickel quenched and tempered steel grade ASTM A553 Type 1 (EN10028-4 X8Ni9+QT640, heat treatment variant with minimum tensile strength of 640 MPa) with 14.5 mm plate thickness. The average measured mechanical properties of the plates were 720 MPa tensile strength, 197 J impact absorbed energy (2.46 J/mm^2) at -196 °C and 250 HV hardness. The chemical composition of the used steel is shown in Table 1.

Table 1. Chemical composition of used steel X8Ni9+QT640, shown in wt%.

C	Mn	Si	P	S	Cr	Ni	Mo	Cu	Fe
0.07	0.39	0.18	0.006	0.001	0.02	9.1	0.02	0.01	bal.

Argon with a flow rate of 25 l min^{-1} served as a process gas for laser welds and as a back shielding. Sheets of X8Ni9 with machined edges and dimensions of 300 x 100 x 14.5 mm^3 were used for square butt LBW.

2.2. Welding equipment

The welding tests were performed using a 20 kW Yb fiber laser YLR 20000 of IPG. The laser radiation was transmitted through an optical fiber of 200 µm in diameter. The laser optics BIMO of HIGHYAG with a magnification factor of 2.8 and a focal length of 350 mm provided the focus diameter of the laser beam (d_f) of 0.56 mm. The laser optics was mounted on the robot arm. The welding movement was carried out by a robot. The welding sample was clamped on the welding table.

2.3. Procedure

Previous studies showed that the cooling time ($\Delta t_{8/5}$) measured in the HAZ and at the root side of the LBW or HLAW welds on thick sheets made of high-strength steels is quite short and can be less than 1.0 s depending on the heat input from the welding process [16, 17]. For this reason, a strategy to increase the cooling time $\Delta t_{8/5}$ or to reduce the cooling rate (°C s^{-1}) was considered to be effective.

For the welding tests discussed here, the samples were preheated before welding with a defocused laser beam. This method was relatively easy to implement by simply removal the welding optics from the specimen surface. Then, the defocused laser beam was moved in a square path over the welding sample in repeated runs. Temperature measurements were done on the root side of the specimens to check whether the sample has reached the desired preheating temperature (T_p). For this purpose, type K thermocouples were placed at a distance of approx. 1 mm to 1.5 mm from the joint, which also made it possible to record the welding thermal cycle in the immediate vicinity of the fusion zone (FZ). When the predefined T_p was reached, the welding process was conducted. The delay between the last preheating run and the start of the welding process was kept below 30 seconds, to prevent the cooling of the weld specimen before welding. A schematic representation of the preheating process with a defocused laser beam can be seen in Fig. 1.

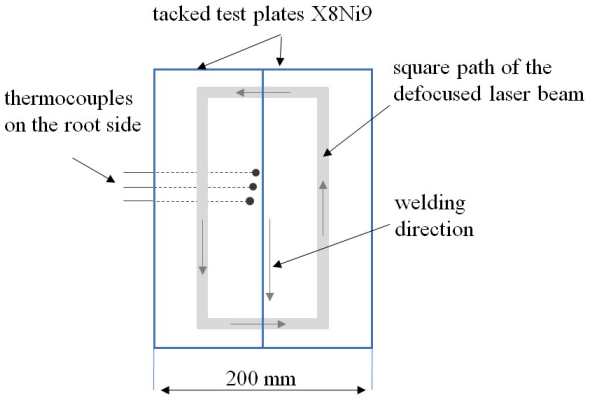

Fig. 1. Schematic representation of the preheating process with a defocused laser beam.

The preheating and welding parameters are shown in Table 2.

Table 2. Preheating and welding parameters.

Parameter	P_L in kW	V in m/min	Focus position Δz / diameter d_f in mm	Number of preheating runs	T_p in °C
Preheating	3.0	0.5	200 / 14.6	2, 3, 4	150, 200, 250
Welding	17.0	2.0	-5 / 0.63		

3. Results

3.1. Laser beam welding with preheating

It was relatively complex to maintain an exact target preheating temperature with the selected preheating method. Therefore, the welding samples were welded at actual temperatures of 160 °C (weld W01), 210 °C (weld W02) and 250 °C (weld W03). In addition, a reference weld W04 was made without preheating at room temperature RT 28 °C. Since the process parameter during preheating were kept constant, the preheating temperature T_p could be raised by increasing the number of preheating runs of the welding head. The temperature curves in Fig. 2, which were measured on the underside of the weld samples, illustrate the warm-up progress for different numbers of preheating runs and the corresponding welding thermal cycles.

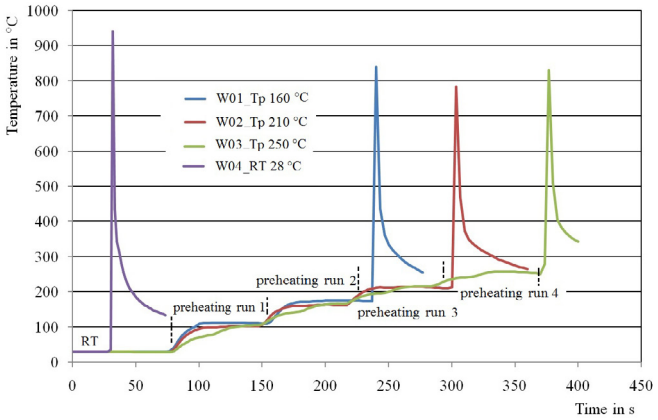

Fig. 2. Welding thermal cycles and preheating temperature progress depending on the number of the preheating runs.

The measured cooling times $\Delta t_{8/5}$ depending on the preheating temperature are summarized in Table 3.

Table 3. Cooling conditions of the laser welds depending on the preheating temperature.

Weld	Number of preheating runs	Measured preheating temperature T_p in °C	Measured cooling time $\Delta t_{8/5}$ in s	Cooling rate in °C s^{-1}
W01	2	160	2.1	142
W02	3	210	2.3	130
W03	4	250	2.9	103
W04	-	-	0.97	309

3.2. Metallographic evaluation

The macrostructure of the welds was observed using an optical light microscope. The specimens were etched with 2% nitric acid in alcohol (Nital). Fig. 3 shows optical macrographs of the cross sections taken from LBW joints produced using laser power P_L 17 kW and welding velocity V 2 m min^{-1} under different preheating conditions. The effect of preheating can be seen in the increase in the width of the FZ and HAZ. The greatest difference can be observed when comparing weld W04 (Fig. 3a) that was carried out without preheating and W03 (Fig. 3d) that was carried out with T_p 250 °C. Thus, while the width of the FZ increases from 1.4 mm to 1.8 mm (factor 1.28), the width of the HAZ increases from 0.75 mm to 1.6 mm (factor 2.13). The same tendency can be observed when comparing welds W01 (Fig. 3b) and W02 (Fig. 3c).

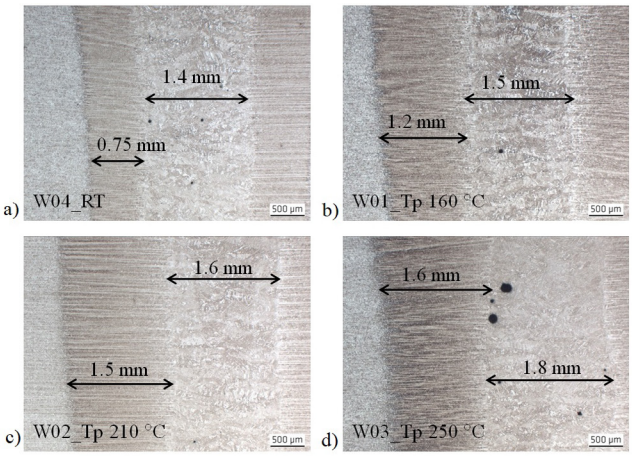

Fig. 3. Macro sections of laser beam welds for different preheating conditions: (a) RT 28 °C; (b) T_p 160 °C; (c) T_p 210 °C and (d) T_p 250 °C.

3.3. Hardness measurement

The hardness HV0.5 was measured with the Zwick 3202 low load hardness tester and calculated according to DIN EN ISO 6507-1. The hardening is characteristic of both the preheated laser welds (W01, W02, W03) and the reference weld without preheating (W04). The relatively high hardness in WM of all the samples confirms that the microstructure of all the cooling rates is martensite. A closer look at the hardness profiles in Fig. 4 shows differences in hardness levels across the HAZ areas for different preheating situations. The reference weld W04 performed at RT shows a hardness peak in the HAZ that reaches 405±10 HV0.5. For the weld seams W01 and W02 performed with preheating, the hardness in the HAZ is in the range between 350...370±10 HV0.5. For the weld W03 done with the highest preheating temperature of 250 °C, the hardness in the HAZ reaches also 370±10 HV0.5, but it is noteworthy, that the width of the HAZ is noticeably increased. This observation also correlates with the measurements in Fig. 3.

3.4. V-notch impact toughness test

The Charpy V-notch impact test was carried out according to DIN EN ISO 148-1 at the test temperature -196 °C. Standard Charpy V-notch samples with the notch location in the middle of the laser WM were used. Five specimens for each weld were tested. The results obtained are shown in Fig. 5.

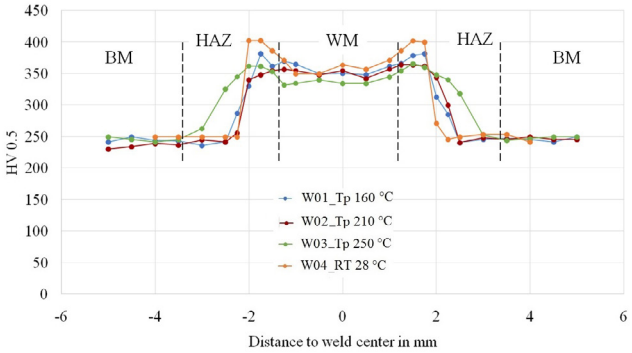

Fig. 4. Hardness profiles for the laser welds performed with different preheating temperatures.

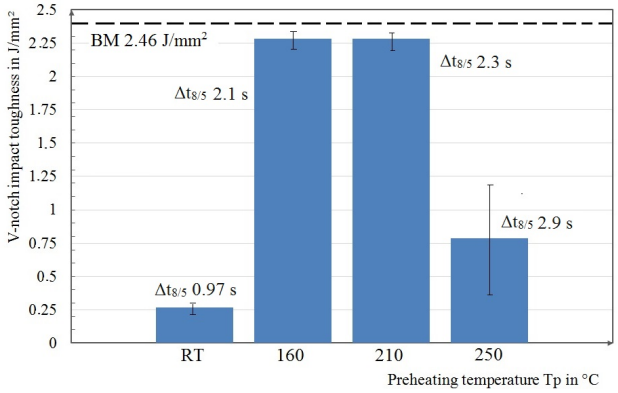

Fig. 5. V-notch impact toughness of laser welds depending on preheating temperature T_p and cooling time $\Delta t_{8/5}$.

The weld W04 ($\Delta t_{8/5}$ 0.97 s) shows the lowest impact toughness value of 0.27±0.05 J/mm², what is under the acceptance level of 0.75 J/mm². The preheated welds W01 ($\Delta t_{8/5}$ 2.1 s) and W02 ($\Delta t_{8/5}$ 2.3 s) show a drastically increase in the impact toughness values, which are 2.28±0.1 J/mm² and 2.25±0.1 J/mm², correspondingly. The preheated weld W03 ($\Delta t_{8/5}$ 2.9 s) has an average impact toughness of 0.76±0.3 J/mm². However, there were isolated lower values of the impact toughness in the range of 0.30 J/mm² to 0.35 J/mm² for the laser weld W03, which contributed to the large scatter of test results. The characteristic examples of fracture surfaces can be seen in Fig. 6.

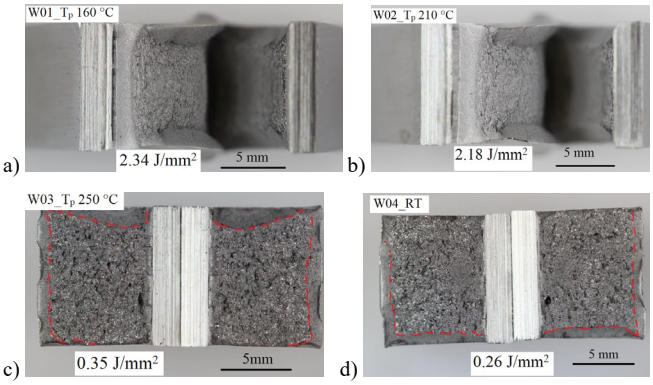

Fig. 6. V-notch impact test fractured specimens for different preheating conditions: (a) T_p 160 °C; (b) T_p 210 °C; (c) T_p 250 °C and (d) RT 28 °C

It should be noted that the tested specimens W01 (Fig. 6a) and W02 (Fig. 6b) exhibit ductile fracture mode with a deviation of the path fracture from WM to BM. This effect is known at the narrow laser beam welds as “fracture path deviation” (FPD) [18]. The fracture surfaces of test samples W03 (Fig. 6c) and W04 (Fig. 6d) show features of a mixed fracture mode with a proportion of ductile to brittle fracture surface of 16%/84% and 11%/89%, respectively.

4. Discussion

The main characteristic of the results achieved is that there is a parameter window at the LBW of thick sheets X8Ni9 in which high notch impact toughness of the weld seams can be achieved. Although all the tested weld seams have a martensitic structure in the WM, they behave differently in the impact test, depending on the welding thermal cycle or cooling time $\Delta t_{8/5}$ and corresponding cooling rate. Such differences in the impact toughness of the welds can be explained by the width of the FZ as well as grade of mechanical properties mismatch between the FZ and HAZ, which was indirectly confirmed by hardness measurements.

The high Charpy toughness of the preheated welds W01 and W02 is due to the fact that the fracture takes place with FPD, whereby a certain volume of the BM is involved in the deformation process. This observation is in accordance to the results of the study [18] in which the authors list some reasons of the FPD formation. These are narrowness of the laser FZ and small volume of the WM involved in deformation process, asymmetry of the stress concentrator because of specific FZ form and the presence of zones in the weld with softer metal. Similar conditions exist for the weld seams W01 and W02: the weld is narrow and unsymmetrical plastic straining between WM and BM favors the crack directly starts to deviate from the notch root into a softer BM over full thickness of the specimen. In contrast, the hardness profile of weld W04, which was carried out without preheating, shows hardness peaks in the HAZ, which prevent the fracture scenario with FPD in the direction of the soft BM. In this case the fracture occurs through the hard laser WM, which is quite brittle due to the short cooling time $\Delta t_{8/5}$ 0.97 s and has a low toughness.

The hardness profile of the weld W03, what was done with the highest T_p 250 °C, does not show any pronounced hardness picks in the HAZ, but the weld has a wider hard zone. In this case, no significant unsymmetrical plastic straining in vicinity of the notch root can be generated, so that the subsequent crack propagates through the laser WM without FPD.

5. Conclusion

The laser beam welding of thick sheets X8Ni9 can lead to a deterioration in the impact strength of the weld seams due to the specific nature of the welding process. A complex microstructural composition of the base metal in combination with unfavorable welding thermal cycles with short cooling times $\Delta t_{8/5}$ of less than 1 s means that the cryogenic impact toughness of the laser welds can fall below the acceptance level for LNG projects, which is 0.75 J/mm².

As a solution to this problem, a parameter window was identified where a sufficiently high impact toughness values comparable to that of the base metal could be reproducibly achieved.

The highest impact toughness up to 2.28±0.1 J/mm² was obtained at the preheating temperature range between 160 °C and 210 °C and cooling times $\Delta t_{8/5}$ 2.1 s and 2.3 s, accordingly. A preheating temperature above 250 °C ($\Delta t_{8/5}$ 2.9 s) is not recommended because a wider hardened area with poor toughness will form.

In other words, impact toughness is influenced not only by the fusion zone microstructure but also by the size of the hardened area as well as the degree of mechanical properties mismatch, as a function of the preheating and welding thermal cycle.

The reduced fusion zone as well as narrow heat affected zone without pronounced hardness peaks is for considerable importance for achieving of high impact toughness of laser beam welded thick plates made of cryogenic X8Ni9 steel.

Acknowledgements

The results presented are part of the research that was carried out within the joint innovative project (GERF ID5111-Egypt and 01DH14012-Germany) between Central Metallurgical Research and Development Institute (CMRDI) of Egypt and Fraunhofer IPK of Germany. The project was supported by the Science and Technology Development Fund (STDF) of the Arab Republic of Egypt and the Federal Ministry of Education and Research (BMBF) of the Federal Republic of Germany.

References

[1] Hoshino, M., Saitoh, N., Muraoka, H., & Saeki, O. (2004). Development of super-9% Ni steel plates with superior low-temperature toughness for LNG storage tanks. Shinnittetsu Giho, 17-20.

[2] Kern, A., Schriever, U., & Stumpfe, J. (2007). Development of 9% nickel steel for LNG applications. steel research international, 78(3), 189-194.

[3] DVS 0955 (02/1999) Schweißtechnische Verarbeitung nickellegierter Stähle für Tieftemperaturanwendungen.

[4] Heinemann J, Einsatz von Nickelbasis Schweisszusatzwerkstoffen im Tankbau, Schweißtechnik Soudure, 01/2010, 16-20.

[5] Wu, Y., Cai, Y., Wang, H., Shi, S., Hua, X., & Wu, Y. (2015). Investigation on microstructure and properties of dissimilar joint between SA553 and SUS304 made by laser welding with filler wire. Materials & Design, 87, 567-578.

[6] Wu, Y., Cai, Y., Sun, D., Zhu, J., & Wu, Y. (2015). Microstructure and properties of high-power laser welding of SUS304 to SA553 for cryogenic applications. Journal of Materials Processing Technology, 225, 56-66.

[7] Huang, Z., Cai, Y., Mu, W., Li, Y., & Hua, X. (2018). Effects of laser energy allocation on weld formation of 9% Ni steel made by narrow gap laser welding filled with nickel based alloy. Journal of Laser Applications, 30(3), 032013.

[8] El-Batahgy, A. M., Gumenyuk, A., Gook, S., & Rethmeier, M. (2018). Comparison between GTA and laser beam welding of 9% Ni steel for critical cryogenic applications. Journal of Materials Processing Technology, 261, 193-201.

[9] Gook, S., El-Batahgy, A., Gumenyuk, A., & Rethmeier, M. (2019). Hybrid laser arc welding of thick plates X8Ni9 for LNG tank construction, Lasers in Manufacturing Conference LiM2019, Munich, Germany

[10] DNVGL Maritime (2017) 'Rules for classification - part 2 materials and welding'

[11] Strömberg, J., & Pak, S. S. H. Cost Efficient LNG Storage Tank Constructed by High Productivity Welding. ESABPO-30, Gothenburg.

[12] Jang, J. I., Ju, J. B., Lee, B. W., Kwon, D., & Kim, W. S. (2003). Effects of microstructural change on fracture characteristics in coarse-grained heat-affected zones of QLT-processed 9% Ni steel. Materials Science and Engineering: A, 340(1-2), 68-79.

[13] Nako, H., Okazaki, Y., Takeda, H., Suenaga, K., & Nakanishi, K. (2010). Comparison of Microstructures at As Welded Zone and Reheated Zone in 9% Ni Steel Similar Composition Weld Metal. In Materials Science Forum (Vol. 638, pp. 3693-3698). Trans Tech Publications.

[14] Barrick, E. J., Jain, D., DuPont, J. N., & Seidman, D. N. (2017). Effects of heating and cooling rates on phase transformations in 10 wt pct Ni steel and their application to gas tungsten arc welding. Metallurgical and Materials Transactions A, 48(12), 5890-5910.

[15] Khourshid, A. E. F. M., & Ghanem, M. A. (2013). The influence of welding parameters on brittle fracture of liquefied natural gas storage tank welded joint. Materials Sciences and Applications, 4(03), 198.

[16] Turichin, G., Kuznetsov, M., Pozdnyakov, A., Gook, S., Gumenyuk, A., & Rethmeier, M. (2018). Influence of heat input and preheating on the cooling rate, microstructure and mechanical properties at the hybrid laser-arc welding of API 5L X80 steel. Procedia Cirp, 74, 748-751.

[17] Wang, G., Wang, J., Yin, L., Hu, H., & Yao, Z. (2020). Quantitative Correlation between Thermal Cycling and the Microstructures of X100 Pipeline Steel Laser-Welded Joints. Materials, 13(1), 121.

[18] Ohata, M., Morimoto, G., Fukuda, Y., Minami, F., Inose, K., & Handa, T. (2015). Prediction of ductile fracture path in Charpy V-notch specimen for laser beam welds. Welding in the World, 59(5), 667-674.